Not so sterile after all: The endomicrobiome of plerocercoids of the cestode parasite *Schistocephalus solidus* and changes to the microbiome of its Threespine Stickleback host.

Megan Hahn, Nolwenn Dheilly

School of Marine and Atmospheric Sciences, Stony Brook University, 100 Nicolls Road, Stony Brook NY, 11774

Abstract

Despite the growing recognition of the role of bacteria in animal biology, the microbiome of parasites remains largely unexplored. In particular, the presence of bacteria in tapeworms has never been investigated and parasites that exit the intestine would be considered sterile. We characterized for the first time the microbiome of a tapeworm. *Schistocephalus solidus* plerocercoids, collected from the body cavity of its stickleback host, were found to harbor a complex microbiome. The most abundant and the most prevalent bacteria was *Polynucleobacter sp*.. In addition, *S. solidus* infection was associated significant changes in the stickleback host gut microbiome with an increase in microbial load and changes in diversity and composition. Finally, the same bacteria were often found in *S. solidus* and the stomach and intestine of the corresponding hosts, a result that highlights the importance of characterizing the microbiome of host tissues and parasites from the same individuals to assess the potential for horizontal transmission of microbes. This study clearly emphasizes the need for further characterization of the microbiome of a broad range of parasites and for studies to determine the ecological, evolutionary and functional role that microbes play in host-parasite interactions.

Key words: Microbiome, microbiota, symbiosis, parasite, helminth, cestode, tapeworm

Introduction

The growing recognition of the fundamental role of microbes in animals and plant biology is changing our understanding of life. The holobiont is defined as the combination of host, and all its associated microbes [1]. We are only starting to comprehend the potential of applying these concepts to host-parasite interactions to decipher the role of host-microbe, parasite-microbe, and host-parasite-microbe interactions in the ecology and evolution of parasites [2]. Microbes provide crucial services to the host, including disease resistance. For instance, there is considerable evidence of the defensive role of bacterial symbionts in insects [3-6]. We are now able to take advantage of this property and resistant mosquitoes carrying the endosymbiotic bacterium *Wolbachia* are being engineered and released in natural populations to reduce the spread of diseases such as malaria, dengue, and Zika [7-12]. In vertebrates too, there is growing evidence that the microbiome participates in resistance mechanisms against diseases. For example, the disruption of the host microbiome at early life-stages, or just before infection can increase the susceptibility to diseases [13-15] and transplantation of the microbiome of resistant individuals into susceptible individuals is sufficient to provide protection[16].

Given the various direct and indirect roles of microbes in host defense, chances are that parasites have gained the ability to take advantage of microbes to increase their virulence. Indeed, evolutionary theories predict that parasite counter-defense strategies are shaped by the host defense mechanisms that they encounter at the time of infection, which explains the major role of immune evasion, and of manipulation of immune pathways in parasite virulence mechanisms [17]. Alteration of the host microbiome has been associated with parasitic helminth infection in various species including pigs, hamsters, cattle, goats, and sheep [18-24]. In rats, infection by the cestode *Hymenolepis diminuta* results in a shift from *Bacilli* to *Clostridia* species [25]. The liver fluke *Opisthorchis viverrini*, associated with hepatobiliary diseases and cholangiocarcinoma, modifies its host intestinal microbiome and promotes *Helicobacter pylori* infection in the liver [26-28]. Similar effects were observed when studying natural populations. For instance, infection by soil transmitted nematodes *Trichuris spp.* in human individuals in Malaysia is correlated with an increased microbial diversity in the gut and a differential abundance of a subset of OTUs, with enrichment in the family *Paraprevotellaceae* [24]. Kreisinger et al.[29] showed that alterations of the gut microbiome composition are species specific; wild mice (*Apodemus flavicollis*) naturally infected by three different helminths (the nematodes *Heligmosomoides polygyrus* and *Syphacia spp.*, and the cestode *Hymenolepis spp.*) had significantly different microbiomes. However, all these studies focused on parasites' alteration of the microbiome of the tissue within which the parasite resides. Here, we characterized the stomach and intestine microbiomes of Threespine sticklebacks (hereafter stickleback), *Gasterosteus aculeatus*, parasitized or not with the cestode parasite *Schistocephalus solidus*. Within 24 hours after ingestion of an infected copepod, *S. solidus* passes through the intestine wall and reaches the body cavity of the fish where it matures into an adult worm, infective for birds [30]. Thus, *S. Solidus* directly interacts with the gut microbiome of the stickleback for a brief period. In the body cavity *S. solidus* may, however, impact the host microbiome indirectly by modulating the expression of immune response genes [31-33].

Parasites can also carry microbes that may participate in their virulence mechanisms [34]. However, studies have so far focused on few bacterial genera of interest. Indeed, it is well known that parasitic nematodes can carry the symbiotic bacteria *Wolbachia* that participate in associated diseases, and can be necessary for the parasite to complete its life cycle [35]. In fact, the causative

agents of lymphatic filariasis and onchocerciasis, two of the most severe and widespread helminth-caused diseases, are associated with *Wolbachia* [36, 37]. Similarly, Digenean trematodes are host of obligate intracellular bacteria of the genus *Neorickettsia*. For instance, *Acanthatrium* sp. and *Lecithodendrium* sp. are vectors of *Neorickettsia risticii* responsible for Potomac Horse fever and the intestinal fluke *Nanophyetus salmincola* is a vector of *Neorickettsia helminthoeca*, that causes Salmon poisoning disease [38, 39]. We found only two examples of characterization of a helminth complete microbiome using a 16S amplicon-based metagenomics approach. The nematode *H. polygyrus* was found associated with a complex microbiome, but it is unclear from this study if the identified microbes were contamination from the environment of the nematode, the highly similar host ileal microbiome [40]. Similarly, the liver fluke *O. viverrini* has recently been found associated with a diverse community of microbes [26]. This discovery has triggered significant interest in *O. viverrini* interactions with microbes and more recent studies suggest that horizontal transmission of microbes to the host may be responsible for associated liver diseases [41-43]. However, it seems that the microbiome of cestode parasites has never been investigated. Here we characterized for the first time the microbiome of the tapeworm, *S. solidus*, while it matures in the body cavity of its fish host, thus limiting the potential for contamination from the host microbiome. We also compared the composition of the microbiome of *S. solidus* with the microbiome of its stickleback host in order to investigate the potential for horizontal transmission of microbes during the first few hours of infection, when the parasite transits through the stomach and intestine.

Results

Discovery of cultivable bacteria in *S. solidus*

As an initial approach to investigate the presence of bacteria in *S. solidus*, we used a culture-based approach. Swabbing *S. solidus* plerocercoids dissected from the body cavity of Threespine Sticklebacks directly on the agar yielded no cultivable strains (Figure 1A). However, we did observe bacteria in our homogenates of the plerocercoids, suggesting that the parasite harbors an endo-microbiome (Figure 1B). Additionally, appreciable differences were noted between the microbiome of *S. solidus* and the stomach and intestine samples of *G. aculeatus* indicating that *Schistocephalus solidus* may harbor a distinct microbiome from its host (Figure S1).

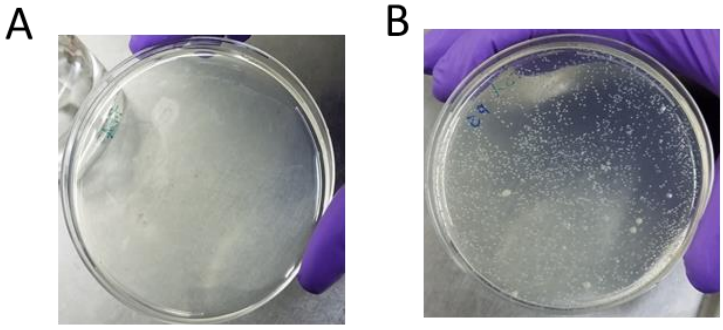

Figure 1: *S. solidus* microbiome and changes to the microbiome of its stickleback host. A. absence of cultivable bacteria on the surface of *S. solidus*. B. presence of cultivable bacteria within *S. solidus*.

Bacterial load

To confirm the presence of bacteria in *S. solidus* and investigate the relationship between bacteria abundance in the fish host and *S. solidus* infection, we used a quantitative PCR (qPCR)

approach with two sets of universal primers targeting the bacteria 16S rRNA gene (Figure S2). Bacteria were present in *S. solidus* samples in measurable quantities, but bacterial load remained significantly lower than in parasitized fish hosts ($p<0.05$, Figure 2). Stomachs and intestines of parasitized sticklebacks had significantly higher bacterial load than non-infected sticklebacks ($p<0.05$, Figure 2, Figure S2).

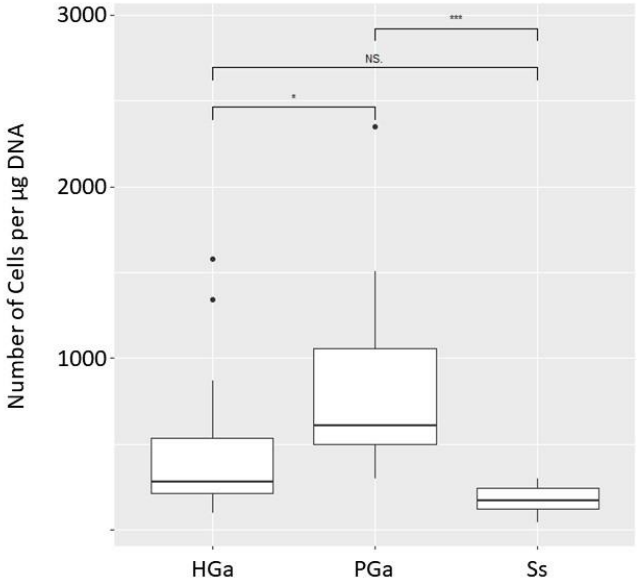

Figure 2: Stickleback and *S. solidus* microbial load. Bacterial load in non-infected *G. aculeatus* (HGa), *S. solidus* (Ss) and parasitized *G. aculeatus* (PGa).

Microbial diversity

The bacterial community composition and diversity was determined by sequencing of the bacterial 16S rRNA gene V4 hypervariable region. Sequencing yielded an average of 10,800 (±SE 8,824) and 43,645 (±SE 16,027) high quality paired-end reads for the *S. solidus* and *G. aculeatus* tissue samples, respectively. Sequencing depth of control samples, i.e. swabs of the body cavity of *G. aculeatus* and surface bacteria from *S. solidus*, was higher and yielded an average of 89,679 (±SE 13,398) high quality reads. We resolved Amplicon Sequence Variants (ASVs) to avoid applying the arbitrary 97% threshold that defines molecular OTUs but has limited biological meaning[44]. The most abundant 100 ASVs in *S. solidus* and *G. aculeatus* represented a cumulative average of 95.1% (±SE 4.9) and 99.1 % (±SE 1.2) of the paired-end reads in the *S. solidus* and *G. aculeatus* tissue samples whereas it represented 26.6 % (±SE 0.9) reads in control samples. Conversely, the top 100 ASVs in control samples (swabs of the body cavity of *G. aculeatus* and "surface" microbiome of *S. solidus*) represented a cumulative average of 90.7% (±SE 1.4) of the paired-end reads in control samples, and only 23.6% (±SE 1.2) and 37.6% (±SE 1.2) of the paired-end reads in the *S. solidus* and *G. aculeatus* tissue samples, respectively. ASVs abundant in control samples were extremely similar to common bacterial contaminants of the MoBio kit used for bacterial DNA extraction and were removed from the analysis[45]. ASVs that were removed as contaminants can be found in Table S1.

Alpha and beta diversity values were calculated on an ASV table rarified to 3,000 reads to compare *G. aculeatus* and *S. solidus* samples, and rarefied to 10,000 reads to compare *G. aculeatus* samples with each other (Figure 3, Table 1, Table S2 Figures S3 and S4). Surprisingly, *S. solidus* had significantly greater alpha diversity when accounting for phylogenetic relatedness,

and greater eveness than its stickleback host (p<0.01 Figure 3, table 1). Comparisons between non-infected and parasitized individuals yielded significant differences in alpha diversity values at both the 3000 and 10,000 rarefaction levels for Faith's Phylogenetic Diversity (p<0.01, Figure S3 and S4). No significant differences were observed between stomach and intestine samples at the 3000 rarefaction level (Table 1), however, significant differences in Shannon diversity were observed at the 10,000 rarefaction level (p<0.05, Table S2, Figure S4).

Table 1: Results of pairwise Kruskal-Wallis H-tests on alpha diversity metrics of bacterial communities for all sample groupings including *G. aculeatus* (Ga), *S. solidus* (Ss), intestine (In), stomach (St), non-infected sticklebacks (H Ga), parasitized sticklebacks (P Ga) at the 3000 rarefaction level.

Comparisons		Evenness		Faith PD		Shannon	
Group 1	**Group 2**	**H**	**p-value**	**H**	**p-value**	**H**	**p-value**
Ga	**Ss**	8.471	0.004*	6.904	0.009*	0.198	0.657
H Ga	**P Ga**	0.963	0.326	7.053	0.008*	0.163	0.686
Ga St	**Ga ln**	1.080	0.299	0.213	0.644	3.524	0.060

* indicates a significant p-value for the given comparison.

Principal coordinate analysis on unweighted UniFrac distances at 3,000 rarefaction depth showed distinct clustering of *S. solidus* and stickleback tissue samples along PCoA axis 1 (paired T-test p<0.05, Figure 3, Table S3) and of non-infected and parasitized sticklebacks along axes 1 and 2 (unpaired T-test p<0.05, Figure 1E). Results obtained with weighted UniFrac distances showed similar significant clustering along axis 1 (Figure S5, Table S4).

Additionally, using 10,000 rarefaction depth to compare stickleback samples confirmed the significant clustering of non-infected and parasitized tissue samples along PC1 (weighted and unweighted UniFrac distance, unpaired t-test p<0.05, Figures S6 and S7, Tables S5 and S6) and of intestine and stomach samples (Weighted UniFrac; PC2, paired t-test p<0.05 Figure S6, S8 and S9, Table S5, Unweighted UniFrac; PC4 and PC17 paired t-test p<0.05, Table S6).

Community dissimilarity metrics (Table S7) further confirmed that *S. solidus* microbial communities were significantly different from *G. aculeatus* samples (PERMANOVA; weighted UniFrac p<0.005, unweighted UnifFrac p<0.005). Most interestingly, *S. solidus* microbial communities were more similar to each other than stickleback samples were to each other (PERMDISP; weighted UniFrac p <0.05, unweighted UniFrac p <0.01). At both the 3,000 and 10,000 rarefaction levels, non-infected and parasitized individuals were observed to host significantly different microbiomes (PERMANOVA; weighted UniFrac P<0.05; unweighted UniFrac P<0.005) with significant differences in dispersion (PERMDISP; weighted UniFrac p<0.05, unweighted UniFrac p<0.05). No significant differences were observed between stomach and intestine samples.

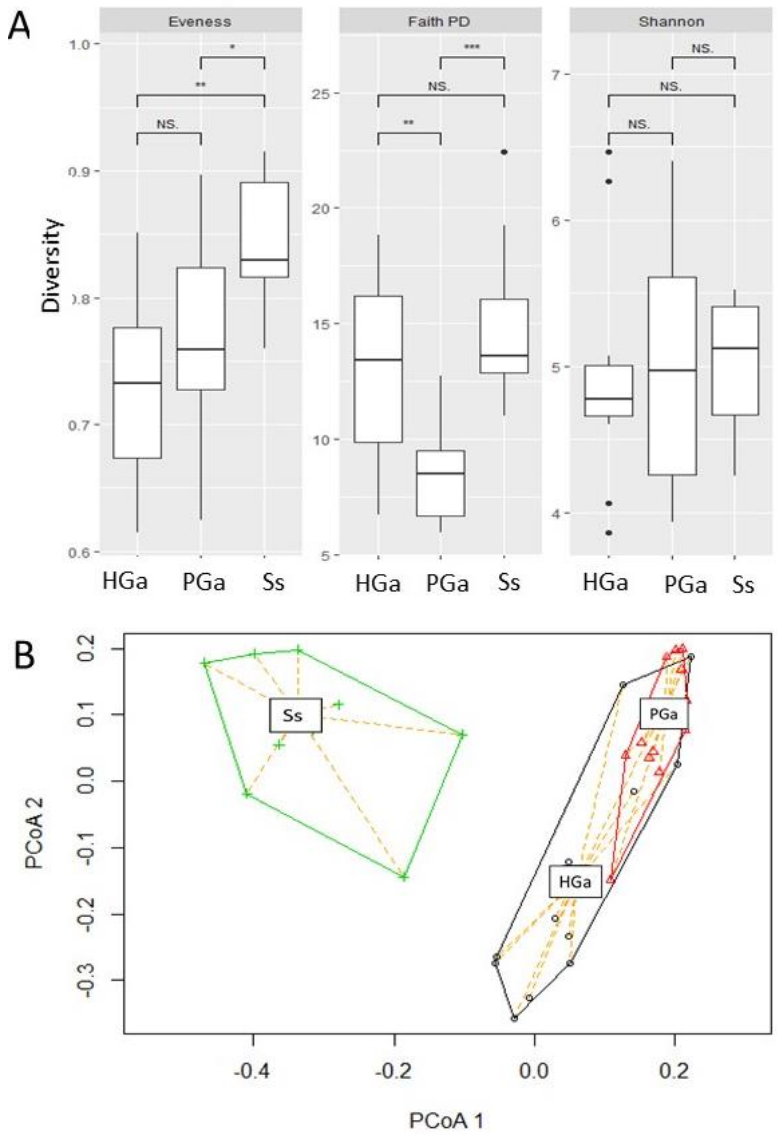

Figure 3: Stickleback and *S. solidus* alpha diversity and principal coordinates analyses. A. alpha diversity values in HGa, Ss and PGa. B. Principal coordinates analysis based on Unweighted Unifrac distance at 3000 rarefaction level.

Taxa distribution and differential abundance analysis

We used DESeq2 to identify bacteria phylotypes differentially abundant among samples. The microbiome of *S. solidus* was significantly different from the microbiome of its host (Table S8, S9, Figure 4 and Figure 5). The proportion of ASVs differentially abundant between *S. solidus* and *G. aculeatus* (84 ASVs, 29 genera, Table 2) was higher than the proportion of ASVs differentially abundant between non-infected and parasitized *G. aculeatus* (44 ASVs, 1 genus, Table 2), between intestines and stomachs of *G. aculeatus* (43 ASVs, 4 genera, Table 2), or between non-infected and parasitized individuals that showed different patterns in stomach and intestine (48 ASVs, 3 genera, Table 2).

Table 2: Number of differentially abundant ASVs/genus identified by DESeq2 (Adj p value <0.05).

Comparison between A	Comparison between B	Total	More in A	More in B
G. aculeatus	***S. solidus* (Ss)**	84 /29	81 / 25	3 / 4
Healthy (H)	**Parasitized (P)**	44 / 1	22 / 1	22 / 0
Intestine (In)	**Stomach (St)**	43 /4	8 / 1	35 / 3
Infection Status:Tissue Interaction		48 / 3		

Some genera of significance in our dataset displayed a great diversity in ASVs resulting in unique ASV being abundant in too few samples to reveal significant differences in abundance whereas at the genus level, the bacteria phylotype appeared differentially abundant. This was particularly noticeable for *Polynucleobacter* bacteria associated with *S. solidus*. Our analysis revealed 29 bacteria differentially abundant between *S. solidus* and *G. aculeatus* (12.6% of all genera), but only four genera were significantly more abundant in *S. solidus* than *G. aculeatus*, and two genera showed high specificity. In particular, 10 variants of *Oxylobacteraceae*, of the genus *Polynucleobacter* and 5 variants of *Rickettsiales* of unknown genera were highly abundant in *S. solidus* (Figure 4). *Polynucleobacter* made up an average cumulative relative abundance of 41% in parasite samples whereas they only made up 4% of the microbial communities found in fish samples (Figure 5). But, at the ASV level, none of the *Polynculeobacter sp.* variants was significantly differentially abundant between *G. aculeatus* and *S. solidus* reflecting the high diversity in abundance among *S. solidus* samples. Similarly, *Ricksettsiales* ASVs represented an average cumulative relative abundance of 8% of the bacteria in parasite samples, but only 0.8% in fish samples, and none of the *Ricksettsiales* ASV was found differentially abundant between fish and parasite samples.

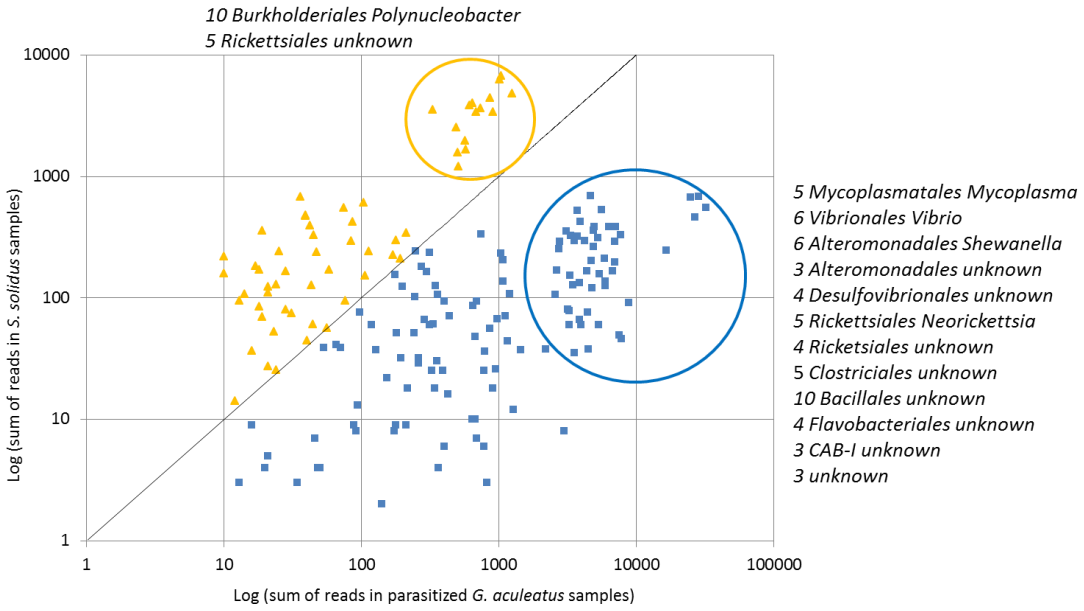

Figure 4: Comparison of the sum of the number of reads in *S. solidus* and corresponding *G. aculeatus* samples. *S. solidus* microbiome is dominated by *Oxylobacteraceae* of the genus *Polynucleobacter* and by *Rickettsiales* of

unknown genus that are present in low abundance in the corresponding fish samples. *G. aculeatus* microbiome is dominated by a great diversity of bacteria that are present in low abundance in the corresponding parasite samples.

Despite the very subtle differences in overall diversity between stomach and intestine samples, significant differences in relative abundance of 43 ASVs were observed, but only 3 genera of low abundance bacteria were significantly affected. Stickleback intestine and stomach microbiome communities were largely dominated by few ASVs of *Clostridiales*, *Rickettsiales, Burkholderiales* and *Desulfovibrionales,* (Figure 5). The cumulative median relative abundance of the five most abundant ASVs in fish microbiome communities represented 56% of the reads, while the next five most abundant ASVs represented 20% of the reads. Seventeen ASVs were found significantly more abundant in intestine than stomach and 26 ASVs were found significantly more abundant in stomach than intestine (Table 2). In particular, stomachs were enriched in various *Gammaproteobacteria* of the order *Alteromonadales,* in *Alphaproteobacteria* of the order *Rickettsiales* and *Sphingomonadales*, and a *Bacilli* of the order *Lactobacillales.* Intestines were enriched in *Clostridia*, of the order *Clostridiales,* and in *Cytophaga* of the order *cytophagale.* Of interest, different sequence variants of *Alphaproteobacteria* of the order *Rhizobiales, Betaproteobacteria* of the order *Burkholderiales*, and *Spartobacteria* of the order *Chtoniobacteriales* were enriched in the intestine and stomach of sticklebacks.

At the genus level, only three low abundance bacteria were found differentially abundant between non-infected and parasitized individuals (Table 2) suggesting that different variants of the same bacteria are found in non-infected and parasitized individuals. Thirty-nine of the ASVs were less abundant in parasitized individuals, with a majority of *Alphaproteobacteria* of the order *Rickettsiales*, *Betaproteobacteria* of the order *Burkholderiales (*including two *polynucleobacter ASVs)*, and *Gammaproteobacteria* of the orders *Alteromonadales* and *Oceanospirillales*. Twenty-two ASVs were more abundant in parasitized individuals including *Clostridia* of the order *Clostridiales*, and *Bacilli* of the order *Bacillales, Alphapoteobacteria* of the order *Rhizobiales* and *Sphingomonadales, Gammaproteobacteria* of the order *Aeromonadales* and *Spirochaetes* of the order *Borreliales*.

On few occasions, individual fish had high abundance of ASVs that only occurred in low abundance in other samples. For example, individual Ga12 (Figure 5) had high abundance of *Gammaproteobacteria* of the family *Shewanella* with a cumulative relative abundance in the stomach and intestine of 31.4% and 41.7%. Yet, the cumulative mean relative abundance across all other fish is 9.2% and 8.7% for the stomach and intestine, respectively. Interestingly, the microbiome of *S. solidus* collected from the same individual was also enriched in these two rare ASVs, with a cumulative relative abundance of 56.2% that contrast with the mean relative abundance of 8.1% in all other parasites.

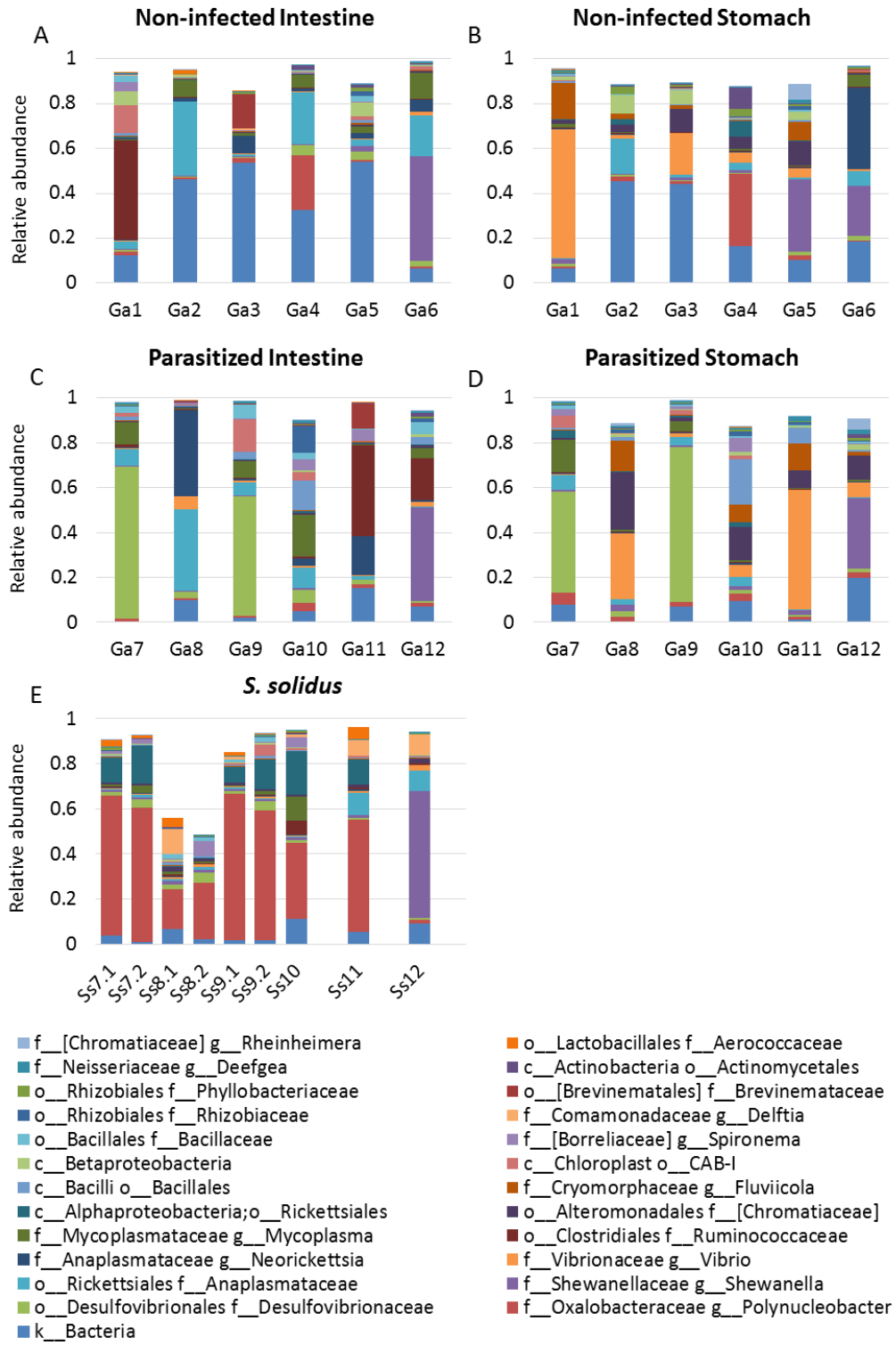

Figure 5: Microbial community diversity characterized in the Intestine (A and C) and Stomach (B and D) of non-infected (A and B, samples Ga1 to 6) and parasitized (C and D, samples Ga 7 to 12) Threespine Sticklebacks and in the corresponding parasite *S. solidus* (E, parasites SS7 to 12. The following number .1 and .2 differentiates parasites collected from the same individual host). The figure represents the relative abundance of the 25 most abundant ASVs. The legend indicates the family (f_) and genus (g_) names.

Polynucleobacter*: a representative of the *Oxylobacteraceae

Polynucleobacter, was the most abundant and the most prevalent bacteria in *S. solidus*. We obtained full length sequence of the 16S gene using direct sequencing[46]. Alignment of the recovered sequence with other *Polynucleobacter* species present in the NCBI database revealed that *S. solidus* associated strain is more related to *P. difficilis* than to other *Polynucleobacter* species (Figure S10).

Discussion

This study revealed for the first time the presence of bacteria associated with a cestode parasite. Previous studies showed that the cestodes *Triaenophorus nodulosus*, *Eubortium rugosum* physically interact with bacteria in the gut of their hosts [47]. Most interestingly, different bacteria were found associated with the microtriches of adult *T. nodulosus* and with the surrounding intestinal environment [48]. However, these studies focused on ectosymbionts, at a life stage where cestodes are surrounded by gut microbes in the intestinal tract of the host. Here, *S. solidus* plerocercoids were collected from the body cavity of *G. aculeatus*. Therefore, the parasite was no longer in contact with the gut microbiota, limiting the potential for contamination. We controlled for the presence of bacteria in the body cavity of the stickleback host, and on the surface of *S. solidus* and confirmed that the fish body cavity is sterile. Using a combination of microscopy observations, culture of cultivable bacteria on agar and 16S amplicon-based sequencing, we demonstrated the existence of a complex endomicrobiome in *S. solidus*. Other helminths have been found to be associated with bacteria. Perhaps the two most famous bacteria known to interact with helminths are *Neorickettsia* and *Wolbachia* which are obligately symbiotic of many trematodes and nematodes respectively[49, 50]. However, investigations regarding these bacteria and their interactions with microbes utilize microscopy, PCR, and direct sequencing approaches that only examine the bacteria of interest leaving other potential microbial symbionts and the parasite microbiome relatively unknown [49, 51-53]. Together with a previous analysis of the microbiome of the liver fluke, *O. viverrini*, this is the second demonstration that helminths may harbor a complex microbiome. This is the first time such bacteria are found in a cestode parasite and the discovery of an endomicrobiome in *S. solidus* suggests that other cestode parasites may also carry microbes. This is highly significant because a broad range of studies have shown that parasite-associated bacteria can interfere with the outcome of infection and/or be responsible for associated diseases following anti-helminth treatments[41, 43, 49, 50, 54, 55]. Tapeworms represent an important problem for health authorities with over 40 species infecting humans as definitive hosts, and 15 during as larval stage, of which many are included in the list of neglected zoonotic diseases by the World Health Organization due to their impact on human health and morbidity[56]. Clearly, the microbiome of helminths of significance for human health should be characterized to leverage the potential for developing new therapeutic strategies [57].

By comparing *S. solidus* microbiome with the microbiome of *G. aculeatus* intestine and stomach, we revealed major differences in composition and diversity. Measures of alpha diversity demonstrated that *S. solidus* microbiome was more diverse than the stickleback intestine and stomach microbiome. Additionally, measures of beta diversity revealed that *S. solidus* microbiome composition is significantly different from *G. aculeatus* gut microbiome. In fact, *S. solidus* samples were more similar to each other than *G. aculeatus* samples were to each other, probably due to the high abundance and prevalence of *Polynucleobacter* ASVs. The most abundant ASVs found in *S. solidus* were all found, albeit in low abundance, in *G. aculeatus.* This

observation could result from cross-contamination during the sample preparation or library preparation as observed in other studies [45, 58, 59]. It could also indicate that many infected individuals had recently ingested a parasitized copepod. But, it could also suggest that *S. solidus* acquire bacteria from its environment while transiting through the host stomach and intestine and before exiting into the body cavity. Such mechanism would result in great inter-individual variations in the microbiome composition of the parasite, dependent upon the composition of the microbiome of its host at the time of infection. This hypothesis is supported by the high similarity in microbiome composition of the plerocercoid Ss12 and corresponding host samples (Ga12) that were enriched with two rare ASVs. Just like vertebrates acquire their microbiome from their environment at birth [60], it is possible that *S. solidus* acquires at least part of its microbiome from its environment when the procercoid loses its outer tegument and cercomer in the stomach and intestine of the host [30].

Another non-mutually exclusive hypothesis is that *S. solidus* acquires microbes from another host or from its environment following egg hatching, or that some bacteria are vertically transmitted. Indeed, bacteria have been observed in eggs of *S. solidus* (Martin Kalbe, personal communications). One such candidate symbiont is *Polynucleobacter sp*. Described species of *Polynucleobacter* include free-living freshwater strains and obligate endosymbionts of ciliates; however, there have been no descriptions to date of a potential *Polynucleobacter*-helminth association [61, 62]. The *Polynucleobacter* species that we discovered in *S. solidus* was more related to *P. difficilis* than to other *Polynucleobacter* species. Our results suggest that we have discovered a new species of endosymbiotic *Polynucleobacter* associated with *S. solidu*s but further studies are necessary to test its presence in the parasite at different life stages. The composition and stability of *S. solidus* microbiome, and potential mixed transmission of bacteria with its intermediate and definitive hosts clearly necessitates further investigation.

By comparing the gut microbiome of non-infected and parasitized individuals, we revealed significant differences. Helminths have been found to impact the gut microbiome of humans and livestock [18-20, 22, 23, 26]. This modification of the host microbiome has been suggested to participate in strategies to impact the host immune system and establish infection [34]. However, these studies focused on intestinal parasites. We found a significant correlation between *S. solidus* infection and *G. aculeatus* microbiome composition, diversity, and total bacterial load. Bacteria more abundant in parasitized individuals do not appear to be transmitted by *S. solidus* because none was significantly more abundant in *S. solidus* than in *G. aculeatus*. Therefore, the correlation between the fish microbiome and infection status could result from two non-mutually exclusive hypotheses: non-infected individuals may carry defensive bacteria that reduce the chance of successful infection by *S. solidus*, or *S. solidus* infection may result in an alteration of the host microbiome. Our study identifies a number of ASVs significantly differentially abundant between non-infected and parasitized individuals that could be targeted in future studies to test these hypotheses using laboratory controlled experimental infections.

Plerocercoids of *S. solidus* were not in contact with the host gut microbiome at the time of sample collection. Therefore, two hypotheses could be explored going forward to determine how *S. solidus* infection might impact its host microbiome. It is possible that *S. solidus* directly interact with stomach and intestine microbes during the first hours of infection, before it transits into the body cavity of the fish. Alteration of the host gut microbiome can have important effects on host fitness and health, including immune and metabolic function [63, 64]. Thus, early alteration of the host gut microbiome at the onset of infection could provide long-term advantages to the

parasite. Alternatively, changes in the fish microbiome composition could result from cross-talks between the microbiome and the immune system. Indeed, *S. solidus* alters different pathways of its host immune system at different time points over the course of an infection [65], that could indirectly impact the fish ability to regulate its microbiome composition. Further studies are therefore necessary to determine at which time point *S. solidus* infection result in changes in the stickleback microbiome. Understanding the role of microbes in helminth virulence and hosts defense responses may reveal vital to understand inter-individual variations in infection success and in host and parasite fitness following successful infections.

It should be noted here that this study focused on field-caught individuals. Given the very high prevalence of *S. solidus* in Cheney lake [66], it is very likely that all non-infected individuals had been exposed to *S. solidus*. As such, parasite exposure, if not parasite infection, probably represents gut homeostasis. It means that more important differences can be expected from future laboratory control experiments focusing on the differences in the microbiome composition of healthy non-exposed sticklebacks, and both exposed but non-infected and successfully infected sticklebacks. To conclude, we also would like to emphasize that, because high parasite prevalence is highly common in field samples of any species, and because this study, and many others have found a significant correlation between parasitism and changes in microbiome composition, regardless of whether the parasite and bacteria are co-localized in the same host tissue. Therefore, the presence of macroparasites in field caught individuals should always be assessed before conducting a study of their microbiome.

Methods

Sample collection

In September 2015, and June 2017 threespine stickleback (*Gasterosteus aculeatus*) specimens were collected live from Cheney Lake in Anchorage Alaska (61° 12' 17" N, 149° 45' 33" W). Fish were caught using un-baited minnow traps placed along the north shoreline of the lake between 0.25 and 2 m deep, and at least 2 m apart. Fish were shipped to Stony Brook University, kept in 20 gallon tanks of 6% seawater at 5°C at the Flax Pond Marine Lab, and fed mysis shrimp twice per day.

Following an acclimation period of 3 weeks fish were euthanized and dissected in sterile conditions. Prior to dissections all surfaces were cleaned with 80% ethanol. Between each subsequent fish dissection, tools and dissecting plate were cleaned with 80% ethanol and betadine to remove potential contaminants. Before dissection, fish were brushed with betadine to prevent contamination of the body cavity with microbes found on the surface of the fish. For dissection, an incision was made along the lateral line of the fish body, around the bony pelvis. The cut extended from the pectoral fins to just anterior of the anus to avoid cutting the intestine. After the initial incision, the bony pelvis was pulled away, opening up the body cavity. Stomach and intestines were either flash frozen in liquid nitrogen for future DNA extraction, or used immediately for bacteria culture. If the fish was parasitized with *S. solidus* the parasite(s) was also taken and either flash frozen, or used immediately for bacteria culture. Swab samples of the body cavity of two non-infecetd and two parasitized individuals were also collected. For two parasitized fish, parasites were shaken in sterile PBS to sample the surface microbiota of *S. solidus.* All samples were then stored at -80°C until use.

Use of experimental animals

The sampling was conducted under Fish sampling permit #SF2015-263 and #P17-025 and fish transport permits #15A-0084 and 17A-0024 provided by the State of Alaska Department of Fish and Game to NMD. Fish were maintained at Stony Brook University under the License to collect or possess #1949 provided by the New York State Department of Environmental Conservation to NMD. Fish experiments were conduct following protocols described in IACUC #237429 and # 815164 to Michael Bell and NMD, respectively. All experiments were performed in accordance with relevant guidelines and regulations.

Culture and isolation of bacteria

In order to culture the microbiome of *S. solidus*, and of the intestine and stomach of *G. aculeatus*, tissue samples were homogenized in PBS, diluted 10 and 100 times and 100µl of liquid was spread evenly on the respective LB and TSA agar plates. Tapeworms isolated from different individual threespine sticklebacks were extensively smeared against both LB and TSA agar to attempt to culture parasite surface bacteria. Bacteria were isolated and cryopreserved in glycerol for future studies.

DNA extraction

Stomach (St) and Intestine (In) collected from six non-infected (HGa) and six parasitized (PGa) sticklebacks were processed further, together with the corresponding nine parasites (Ss). DNA extraction was performed using a MoBIO Powerlyzer Powersoil Kit (Cat#12855) with the following modifications to the manufacturer's protocol. First, all tissue samples were placed in tough tubes with 3mm glass beads. To each tube, we added 750µL of the bead beating solution supplied with the extraction kit. Samples underwent three rounds of 20 sec bead beating cycles and were kept on ice between each round. The homogenate was transferred to the MoBIO supplied 0.1mm bead tube and incubated with 60µL of the provided C1 solution for 10 min at 60°C. After vortexing, centrifugation, and filtration with solution C5 according to manufacturer's protocol, 75µL of solution C6 was added to the spin filter in a clean 2mL tube and incubated at room temperature for 5 min before centrifugation at 10,000g for 30 sec. This final step was repeated to obtain a final DNA extract of 150µL.

RT and real-time qPCR

Bacteria from all samples of fish and parasites were quantified by qPCR using the QuantStudio 6 Flex RT PCR System (Fisher Scientific). Two 16S primers were used (Forward: TCCTACGGGAGGCAGCAGT, Reverse: GACTACCAGGGTATCTAATCCTGTT [67] and Forward: GTGSTGCAYGGYTGTCGTCA, Reverse: ACGTCRTCCMCACCTTCCTC [68]) and compared to an *E. coli* standard for which cell count was obtained using a hepocytometer (Stony Brook, NY). The qPCR mixture (20µL) was composed of 10µL of SYBR green master mix (CAT# 4309155), 4.8µL Molecular biology grade water (CAT#46000), 0.6µL forward primer, 0.6uL reverse primer, and 4µL DNA.

16S rDNA amplification and Illumina MiSeq sequencing

We sequenced the stomach and intestine microbiota from six non-infected and six parasitized individuals in addition to nine parasite microbiomes from the infected individuals. Swabs, PBS, and negative controls from the DNA extraction were also sequenced. The 16S rDNA V4-V5 hypervariable region was amplified with *E. coli* 515f and 806r primers (with barcode on the

forward primer) as specified by the Earth Microbiome Project [69-72]. We used a 28 cycle PCR (5 cycle used on PCR products) using the HotStarTaq Plus Master Mix Kit (Qiagen, USA) under the following conditions: 94°C for 3 minutes, followed by 28 cycles of 94°C for 30 seconds, 53°C for 40 seconds and 72°C for 1 minute, after which a final elongation step at 72°C for 5 minutes was performed. After amplification, PCR products are checked in 2% agarose gel to determine the success of amplification and the relative intensity of bands. Multiple samples are pooled together (e.g., 100 samples) in equal proportions based on their molecular weight and DNA concentrations. Pooled samples are purified using calibrated Ampure XP beads. Then the pooled and purified PCR product is used to prepare illumina DNA library. Sequencing was performed at MR DNA to obtain 250bp paired end reads (www.mrdnalab.com, Shallowater, TX, USA) on a MiSeq following the manufacturer's guidelines. Sequence data were initially processed using MR DNA analysis pipeline (MR DNA, Shallowater, TX, USA). In summary, sequences were joined, depleted of barcodes then sequences <150bp removed, sequences with ambiguous base calls removed.

Microbiome composition analysis with QIIME

The 16S rDNA gene Illumina reads were further processed using methods implemented in QIIME2, Phyloseq [73, 74] and R as detailed in the supplementary information (Supp. File 1). Briefly, samples were demultiplexed and quality filtered. ASVs (amplicon sequence variants) were picked against the Greengene database using the DADA2 pipeline. . The final ASV table was then rarefied to a depth of 3000 sequences per sample for comparisons between the microbiomes of *S. solidus* and stickleback tissue samples, and 10,000 sequences for comparisons among stickleback tissue samples. Rarefaction curves showed that at these depths of sampling, we were able to sample a large portion of the ASV diversity present while still retaining all samples (Supp File 2).

Diversity measures and statistical analyses

Analyses were performed using QIIME2 and the Phyloseq and DESeq2 packages in R [74, 75].Each of the following diversity metrics and statistical analyses were carried out at the 3,000 and 10,000 rarefaction levels to perform comparisons (i) among all sample categories (HGaIn, PGaIn, HGaSt, PGaSt, Ss), between species (all Ga versus Ss; 3,000 only), between tissue (all In vs all St; 10,000 only), and depending on infection status (all HGa versus all PGa; 10,000 only). Pielou's Evenness, Shannon, and Faith's Phylogenic Diversity (PD_Whole_tree, with Greegene taxonomy tree) alpha diversity metrics were used to estimate within species diversity. Alpha diversity was compared between sample types using pairwise Kruskal-Wallis H-tests. Beta diversity was calculated with both weighted and unweighted UniFrac metrics. PERMANOVA at 10,000 permutations was carried out to identify significant differences between categories of samples. We tested for homogeneity of multivariate dispersion using PERMDISP. Principal coordinate analysis (PCoA) was performed to look for patterns in unconstrained multivariate space and a combination of paired and unpaired pairwise t-tests were used to test if axes significantly discriminate groups of samples. DESeq2 was used on raw data to examine differences in individual microbe abundance.

Direct sequencing of *Polynucleobacter sp.*

Polynucleobacter, a genera found to be abundant in parasite samples was investigated using a combination of PCR and direct sequencing. DNA from intestine and parasite samples was amplified using the primers F19 (5'-GAT CCT GGC TCA GAT TGA AC-3') and R1517 (5'-

TGA TCC AGC CGC ACC TTC-3'). Amplicons were cleaned using the MoBIO Ultra-Clean PCR Clean-up Kit (CAT#) and directly sequenced with the primers F7A (5'-AGAGTTTGATCCTGGCTCA-3'), I343 (5'-TACGGGAGGCAGCAG-3'), F1099 (5'-GCAACGAGCGCAACCC-3') and F515 (5'-GTGCCAGCAGCCGCGGT-3). Sequences were analyzed using Seaview4 and Bio Edit. Briefly, sequences were trimmed to remove poor quality ends. Sequences were aligned to *Polynucleobacter* reference sequences obtained from the NCBI database. The highest quality parasite sequence was chosen and a consensus sequence was made based on sequences from the four primers. A phylogenetic tree was then generated in Seaview with PhyML program where non-parametric bootstrapping with 100 replicates was used to determine branch support.

Data Accessibility

All data is being made available through the NCBI database under BioSample accessions SAMN08800217 to SAMN08800225 for *S. solidus* samples and BioSample accessions SAMN08800337 to SAMN08800360 for *G. aculeatus* samples. The 16S sequence of Polynucleobacter from *S. solidus* is available under GenBank accession number MH122759.

8 References

1. Margulis, L. Symbiogenesis and Symbionticism (1991).
2. Dheilly, N.M. Holobiont–Holobiont interactions: redefining host–parasite interactions. *PLoS Pathog* **10**, e1004093 (2014).
3. Oliver, K.M., Russell, J.A., Moran, N.A. & Hunter, M.S. Facultative bacterial symbionts in aphids confer resistance to parasitic wasps. *Proc Natl Acad Sci* **100**, 1803-1807 (2003).
4. Teixeira, L., Ferreira, Á. & Ashburner, M. The bacterial symbiont *Wolbachia* induces resistance to RNA viral infections in *Drosophila melanogaster*. *PLoS Biol.* **6**, e1000002 (2008).
5. Xie, J., Butler, S., Sanchez, G. & Mateos, M. Male killing *Spiroplasma* protects *Drosophila melanogaster* against two parasitoid wasps. *J Hered* **112**, 399 (2014).
6. Hughes, G.L., Koga, R., Xue, P., Fukatsu, T. & Rasgon, J.L. *Wolbachia* infections are virulent and inhibit the human malaria parasite *Plasmodium falciparum* in *Anopheles gambiae*. *PLoS Pathog* **7**, e1002043 (2011).
7. Adams, M.D. et al. The genome sequence of *Drosophila melanogaster*. *Science* **287**, 2185-95 (2000).
8. Aliota, M.T., Peinado, S.A., Velez, I.D. & Osorio, J.E. The wMel strain of *Wolbachia* reduces transmission of Zika virus by *Aedes aegypti*. *Sci Rep* **6**, srep28792 (2016).
9. Dutra, H.L.C. et al. *Wolbachia* blocks currently circulating Zika virus isolates in Brazilian *Aedes aegypti* mosquitoes. *Cell Host Microbe* **19**, 771-774 (2016).
10. Pan, X., Thiem, S. & Xi, Z. in Arthropod Vector: Controller of Disease Transmission, Volume 1 35-58 (Elsevier, 2017).
11. Carrington, L.B. et al. Field-and clinically derived estimates of *Wolbachia*-mediated blocking of dengue virus transmission potential in *Aedes aegypti* mosquitoes. *Proc Natl Acad Sci USA* **115**, 361-366 (2018).
12. Wang, S. et al. Driving mosquito refractoriness to *Plasmodium falciparum* with engineered symbiotic bacteria. *Science* **357**, 1399-1402 (2017).
13. Knutie, S.A., Wilkinson, C.L., Kohl, K.D. & Rohr, J.R. Early-life disruption of amphibian microbiota decreases later-life resistance to parasites. *Nat Commun* **8**, 86 (2017).

14. Theriot, C.M. et al. Antibiotic-induced shifts in the mouse gut microbiome and metabolome increase susceptibility to *Clostridium difficile* infection. *Nat Commun* **5**, 3114 (2014).
15. Schuijt, T.J. et al. The gut microbiota plays a protective role in the host defence against pneumococcal pneumonia. *Gut*, gutjnl-2015-309728 (2015).
16. Rosshart, S.P. et al. 5 (Am Assoc Immnol, 2017).
17. Schmid-Hempel, P. Immune defence, parasite evasion strategies and their relevance for 'macroscopic phenomena'such as virulence. *Philos Trans R Soc Lond B Biol Sci* **364**, 85-98 (2009).
18. Wu, S. et al. Worm burden-dependent disruption of the porcine colon microbiota by *Trichuris suis* infection. *PloS ONE* **7**, e35470 (2012).
19. Li, R.W., Wu, S., Li, W., Huang, Y. & Gasbarre, L.C. Metagenome plasticity of the bovine abomasal microbiota in immune animals in response to *Ostertagia ostertagi* infection. *PloS ONE* **6**, e24417 (2011).
20. Nicholls, C. Endoscopy, physiology and bacterial flora of sheep infected with abomasal nematodes. (1987).
21. Li, R.W. et al. Alterations in the porcine colon microbiota induced by the gastrointestinal nematode *Trichuris suis*. *Infect Immun* **80**, 2150-2157 (2012).
22. Li, R.W. et al. The effect of helminth infection on the microbial composition and structure of the caprine abomasal microbiome. *Sci Rep* **6** (2016).
23. Cantacessi, C. et al. Impact of experimental hookworm infection on the human gut microbiota. *J Infect Dis* **210**, 1431-1434 (2014).
24. Lee, S.C. et al. Helminth colonization is associated with increased diversity of the gut microbiota. *PLoS Negl Trop Dis* **8**, e2880 (2014).
25. McKenney, E.A. et al. Alteration of the rat cecal microbiome during colonization with the helminth *Hymenolepis diminuta*. *Gut Micro* **6**, 182-193 (2015).
26. Plieskatt, J.L. et al. Infection with the carcinogenic liver fluke *Opisthorchis viverrini* modifies intestinal and biliary microbiome. *FASEB J* **27**, 4572-4584 (2013).
27. Chng, K.R. et al. Tissue microbiome profiling identifies an enrichment of specific enteric bacteria In *Opisthorchis viverrini* associated cholangiocarcinoma. *EBioMedicine* (2016).
28. Itthitaetrakool, U. et al. Chronic *Opisthorchis viverrini* Infection Changes the Liver Microbiome and Promotes *Helicobacter* Growth. *PloS ONE* **11**, e0165798 (2016).
29. Kreisinger, J., Bastien, G., Hauffe, H.C., Marchesi, J. & Perkins, S.E. Interactions between multiple helminths and the gut microbiota in wild rodents. *Phil Trans R Soc Biol* **370**, 20140295 (2015).
30. Hammerschmidt, K. & Kurtz, J. *Schistocephalus solidus*: Establishment of tapeworms in sticklebacks–fast food or fast lane? *Exp Parasitol* **116**, 142-149 (2007).
31. Kurtz, J. et al. MHC genes and oxidative stress in sticklebacks: an immuno-ecological approach. *Philos Trans R Soc Lond B Biol Sci* **273**, 1407-1414 (2006).
32. Kurtz, J. et al. Major histocompatibility complex diversity influences parasite resistance and innate immunity in sticklebacks. *Philos Trans R Soc Lond B Biol Sci* **271**, 197-204 (2004).
33. Hammerschmidt, K. & Kurtz, J. Evolutionary implications of the adaptation to different immune systems in a parasite with a complex life cycle. *Philos Trans R Soc Lond B Biol Sci* **272**, 2511-2518 (2005).

34. Dheilly, N.M., Poulin, R. & Thomas, F. Biological warfare: Microorganisms as drivers of host–parasite interactions. *Infect Genet Evol* **34**, 251-259 (2015).
35. Bandi, C., Anderson, T.J., Genchi, C. & Blaxter, M.L. Phylogeny of *Wolbachia* in filarial nematodes. *Philos Trans R Soc Lond B Biol Sci* **265**, 2407-2413 (1998).
36. Dreyer, G., Noroes, J., Figueredo-Silva, J. & Piessens, W. Pathogenesis of lymphatic disease in Bancroftian filariasis: a clinical perspective. *Parasitol Today* **16**, 544-548 (2000).
37. Hoerauf, A. et al. Doxycycline in the treatment of human onchocerciasis: kinetics of *Wolbachia* endobacteria reduction and of inhibition of embryogenesis in female *Onchocerca* worms. *Microb Infect* **5**, 261-273 (2003).
38. Millemann, R.E. & Knapp, S.E. Biology of *Nanophyetus salmincola* and" salmon poisoning" disease. *Adv Parasitol* **8**, 1-41 (1970).
39. Pusterla, N., Johnson, E., Chae, J. & Madigan, J.E. Digenetic trematodes, *Acanthatrium* sp. and *Lecithodendrium* sp., as vectors of *Neorickettsia risticii*, the agent of Potomac horse fever. *J Helminthol* **77**, 335-339 (2003).
40. Walk, S.T., Blum, A.M., Ewing, S.A.S., Weinstock, J.V. & Young, V.B. Alteration of the murine gut microbiota during infection with the parasitic helminth *Heligmosomoides polygyrus*. *J Inflamm Bowel Dis Disord* **16**, 1841-1849 (2010).
41. Deenonpoe, R. et al. The carcinogenic liver fluke *Opisthorchis viverrini* is a reservoir for species of *Helicobacter*. *APJCP* **16**, 1751 (2015).
42. Dangtakot, R. et al. Coinfection with *Helicobacter pylori* and *Opisthorchis viverrini* enhances the severity of hepatobiliary abnormalities in hamsters. *Infect Immun* **85**, e00009-17 (2017).
43. Deenonpoe, R. et al. Elevated prevalence of *Helicobacter* species and virulence factors in opisthorchiasis and associated hepatobiliary disease. *Sci Rep* **7** (2017).
44. Callahan, B.J., McMurdie, P.J. & Holmes, S.P. Exact sequence variants should replace operational taxonomic units in marker-gene data analysis. *ISME* **11**, 2639 (2017).
45. Glassing, A., Dowd, S.E., Galandiuk, S., Davis, B. & Chiodini, R.J. Inherent bacterial DNA contamination of extraction and sequencing reagents may affect interpretation of microbiota in low bacterial biomass samples. *Gut pathog* **8**, 24 (2016).
46. Vannini, C., Ferrantini, F., Ristori, A., Verni, F. & Petroni, G. Betaproteobacterial symbionts of the ciliate *Euplotes*: origin and tangled evolutionary path of an obligate microbial association. *Environ Microbiol* **14**, 2553-2563 (2012).
47. Izvekova, G. & Lapteva, N. Microflora associated with the digestive-transport surfaces of fish and their parasitic cestodes. *Russ J Ecol* **35**, 176-180 (2004).
48. Korneva, Z. & Plotnikov, A. Indigenous microflora associated with the tegument of *Triaenophorus nodulosus* (Cestoda) and the intestine of its pike host. *Parazitologiia* **40**, 535-546 (2005).
49. Taylor, M.J., Bandi, C. & Hoerauf, A. Wolbachia. Bacterial endosymbionts of filarial nematodes. *Adv Parasitol* **60**, 245-284 (2005).
50. Vaughan, J.A., Tkach, V.V. & Greiman, S.E. in Adv Parasitol 253-297 (Elsevier, 2012).
51. Greiman, S.E., Tkach, V.V., Pulis, E., Fayton, T.J. & Curran, S.S. Large scale screening of digeneans for *Neorickettsia* endosymbionts using real-time PCR reveals new *Neorickettsia* genotypes, host associations and geographic records. *PLoS ONE* **9**, e98453 (2014).

52. Fischer, K., Tkach, V.V., Curtis, K.C. & Fischer, P.U. Ultrastructure and localization of *Neorickettsia* in adult digenean trematodes provides novel insights into helminth-endobacteria interaction. *Parasit Vectors* **10**, 177 (2017).
53. Lawrence, S.A. & Poulin, R. Detection of the bacterial endosymbiont *Neorickettsia* in a New Zealand digenean. *J Parasitol Res* **115**, 4275-4279 (2016).
54. Taylor, M.J., Hoerauf, A. & Bockarie, M. Lymphatic filariasis and onchocerciasis. *The Lancet* **376**, 1175-1185 (2010).
55. Taylor, M.J., Cross, H.F. & Bilo, K. Inflammatory responses induced by the filarial nematode *Brugia malayi* are mediated by lipopolysaccharide-like activity from endosymbiotic *Wolbachia* bacteria. *J Exp Med* **191**, 1429-1436 (2000).
56. Moloo, A. (World Health Organization, 2018).
57. Dheilly, N.M. et al. Parasite Microbiome Project: Systematic Investigation of Microbiome Dynamics within and across Parasite-Host Interactions. *mSystems* **2**, e00050-17 (2017).
58. Salter, S.J. et al. Reagent and laboratory contamination can critically impact sequence-based microbiome analyses. *BMC biology* **12**, 87 (2014).
59. Weiss, S. et al. Tracking down the sources of experimental contamination in microbiome studies. *Genome biol* **15**, 564 (2014).
60. Yatsunenko, T. et al. Human gut microbiome viewed across age and geography. *Nature* **486**, 222-227 (2012).
61. Springer, N., Amann, R., Ludwig, W., Schleifer, K.-H. & Schmidt, H. *Polynucleobacter necessarius*, an obligate bacterial endosymbiont of the hypotrichous ciliate *Euplotes aediculatus*, is a member of the β-subclass of *Proteobacteria*. *FEMS Microbiol Lett* **135**, 333-336 (1996).
62. Horn, M. et al. Obligate bacterial endosymbionts of *Acanthamoeba* spp. related to the beta-*Proteobacteria*: proposal of *Candidatus Procabacter acanthamoebae* gen. nov., sp. nov. *Int J Syst Evol Microbiol* **52**, 599-605 (2002).
63. Round, J.L. & Mazmanian, S.K. The gut microbiota shapes intestinal immune responses during health and disease. *Nat Rev Immunol* **9**, 313-323 (2009).
64. Devaraj, S., Hemarajata, P. & Versalovic, J. The human gut microbiome and body metabolism: implications for obesity and diabetes. *Clin Chem* **59**, 617-628 (2013).
65. Scharsack, J.P., Koch, K. & Hammerschmidt, K. Who is in control of the stickleback immune system: interactions between *Schistocephalus solidus* and its specific vertebrate host. *Proc R Soc Lond [Biol]* **274**, 3151-3158 (2007).
66. Bell, M.A. et al. Reintroduction of threespine stickleback into Cheney and Scout Lakes, Alaska. *Evol Ecol Res* **17**, 157-178 (2016).
67. Larsen, N. et al. Gut microbiota in human adults with type 2 diabetes differs from non-diabetic adults. *PloS one* **5**, e9085 (2010).
68. Horz, H., Vianna, M., Gomes, B. & Conrads, G. Evaluation of universal probes and primer sets for assessing total bacterial load in clinical samples: general implications and practical use in endodontic antimicrobial therapy. *J Clin Microbiol* **43**, 5332-5337 (2005).
69. Caporaso, J.G. et al. Ultra-high-throughput microbial community analysis on the Illumina HiSeq and MiSeq platforms. *ISME* **6**, 1621-1624 (2012).
70. Caporaso, J.G. et al. Global patterns of 16S rRNA diversity at a depth of millions of sequences per sample. *Proc Natl Acad Sci USA* **108**, 4516-4522 (2011).

71. Walters, W. et al. Improved bacterial 16S rRNA gene (V4 and V4-5) and fungal internal transcribed spacer marker gene primers for microbial community surveys. *mSystems* **1**, e00009-15 (2016).
72. Parada, A.E., Needham, D.M. & Fuhrman, J.A. Every base matters: assessing small subunit rRNA primers for marine microbiomes with mock communities, time series and global field samples. *Environ microbiol* (2015).
73. Callahan, B.J. et al. DADA2: high-resolution sample inference from Illumina amplicon data. *Nature methods* **13**, 581-583 (2016).
74. McMurdie, P.J. & Holmes, S. Phyloseq: an R package for reproducible interactive analysis and graphics of microbiome census data. *PloS ONE* **8**, e61217 (2013).
75. Caporaso, J.G. et al. QIIME allows analysis of high-throughput community sequencing data. *Nature methods* **7**, 335-336 (2010).

Acknowledgements

We would like to acknowledge the expertise and assistance of Dr. Michael Bell in fish collection and dissection techniques. This project was funded by the Eppley Foundation for Research and the Maze-Landeau Foundation.

Author contributions statement

MA and NMD designed the study. MA completed the analysis with the help of NMD and wrote a first version of the manuscript. NMD reviewed the manuscript. Both authors approve the final version of the manuscript.

Additional information

Supplementary figures and tables are provided in Supplementary file 1.